^1H and ^{15}N Resonance Assignment and Secondary Structure of Capsicein, an α-Elicitin, Determined by Three-Dimensional Heteronuclear NMR

Serge Bouaziz,[‡] Carine van Heijenoort,[‡] Jean-Claude Huet,[§] Jean-Claude Pernollet,[§] and Eric Guittet*[,‡]

Laboratoire de Résonance Magnétique Nucléaire, Institut de Chimie des Substances Naturelles du CNRS, 91190 Gif-sur-Yvette, France, and Laboratoire d'Etude des Protéines, INRA-Versailles Route de St. Cyr, 78026 Versailles Cedex, France

Received December 10, 1993; Revised Manuscript Received April 12, 1994[⊗]

ABSTRACT: The backbone ^1H and ^{15}N resonance assignments and solution secondary structure determination of capsicein, a protein of 98 residues with a molecular mass of 10161 Da, are presented. Capsicein belongs to the elicitin family, elicitor molecules having toxic and signaling properties that are secreted by *Phytophthora* fungi, responsible for the incompatible hypersensitive reaction of diverse plant species leading to resistance against fungal or bacterial plant pathogens. The protein was uniformly labeled with ^{15}N to overcome spectral overlap of the proton resonances. A combination of 3D HOHAHA-HMQC and 3D NOESY-HMQC experiments allowed the identification of spin systems with through-bond correlations, which were in turn correlated by through-space connections. The sequential assignment was obtained for main- and side-chain resonances and led to the identification of all secondary structures. A 3D HMQC-NOESY-HMQC experiment was performed which characterized the NH(i)–NH(i+1) connections specific to α-helical structures. This proved particularly useful for the assignment of degenerate amide protons of successive residues in α-helical structures. The data show five α-helical regions comprising residues 5–18, 26–33, 44–58, 59–67, and 86–98 and a two-stranded antiparallel β-sheet involving residues 70–75 and 80–85, packed around a hydrophobic core grouping all of the aromatic residues. The C-terminal secondary structure motifs of capsicein evoke phospholipase structural features, which suggests that elicitins might interact with the lipidic molecules of the plasma membrane.

Most microorganisms are unsuccessful in establishing themselves as plant parasites due to defense mechanisms controlled by the host during the invasion process. These mechanisms are stimulated by molecules of microorganism origin, generically termed elicitors (Dixon & Lamb, 1990; Hahlbrock et al., 1990), which induce reaction cascades usually resulting in a necrotic hypersensitive response within the host cell (Anderson et al., 1991). Elicitins are both a novel class of protein elicitors and an original family of proteins secreted by the phytopathogenic fungi belonging to the genus *Phytophthora* (Pernollet et al., 1993). They are secreted with removal of a signal peptide (Tercé-Laforgue et al., 1992), penetrate the plant through the root system (Pernollet et al., 1993) and proceed to the leaf cell, where they necrotize without requiring *in planta* biochemical alterations for their activity to develop (Zanetti et al., 1992). They cause leaf necrosis and are responsible for the induction of the hypersensitive reaction, serving as signals for the interaction between plant and *Phytophthora* fungi. They also induce protection against a subsequent inoculation with pathogens (Ricci et al., 1989; Kamoun et al., 1993). Elicitins are 98-residue holoproteins of MW *ca.* 10000 with three disulfide bridges (Nespoulous et al., 1992), which show sequence homology greater than 66% (Nespoulous et al., 1992; Huet et al., 1992; Huet & Pernollet, 1993). The comparison of the complete sequences of 10 elicitins led to their classification into two groups (Pernollet et al., 1993; Nespoulous et al., 1992): the α class corresponds to acidic molecules with a valyl residue at position 13, while the β class is characterized by a hydrophilic residue at that position and a basic isoelectric point. These two classes are also distinguished by their necrotic properties on tobacco leaves since β elicitins are 100-fold more toxic than α ones. As part of an extensive study of these proteins, we first focused on capsicein, one of the α class elicitins (M_r 10161 Da, pI 3.5) (see Figure 1), which has been shown to induce at very low level protection of tobacco against *Phytophthora nicotianae*, the causal organism of tobacco black shank, and is one of the least toxic elicitins (Ricci et al., 1989; Pernollet et al., 1993). The size of the elicitins lends them well to NMR analysis. To date no crystallographic data are available. Structural information about capsicein will allow the design of elicitin-like molecules that are able to stimulate the plant defense responses and to protect against pathogens, but that are devoid of necrotic properties, and will allow the elucidation of the molecular mechanisms involved in the elicitin signaling pathway.

2D NMR[1] spectroscopy has been applied successfully to the three-dimensional structure elucidation of proteins up to 100 amino acids (Wüthrich, 1986). In the case of capsicein, the secondary structures are mainly α-helices, as seen from a 2D NOESY experiment. This is associated with a small vicinal coupling between the amide and the Hα protons, and the 3D homonuclear NMR experiments (Griesinger et al., 1987; Vuister et al., 1988) did not allow a complete assignment of the spectra. NOESY-HMQC experiments (Fesik &

‡ Institut de Chimie des Substances Naturelles du CNRS.
§ INRA-Versailles Route de St. Cyr.
⊗ Abstract published in *Advance ACS Abstracts,* June 1, 1994.

[1] Abbreviations: 2D, 3D NMR, two-dimensional, three-dimensional nuclear magnetic resonance; NOE, nuclear Overhauser effect; NOESY, nuclear Overhauser effect spectroscopy; TOCSY, total correlation spectroscopy; HOHAHA, homonuclear Hartmann–Hahn spectroscopy; TPPI, time proportional phase increment; SCUBA, stimulated cross peaks under bleached alphas; DQF-COSY, double quantum filtered correlation spectroscopy; TQF-COSY, triple quantum filtered correlation spectroscopy; ROE, rotating-frame Overhauser effect; HMQC, heteronuclear multiple quantum correlation; HSQC, heteronuclear single quantum correlation.

0006-2960/94/0433-8188$04.50/0 © 1994 American Chemical Society

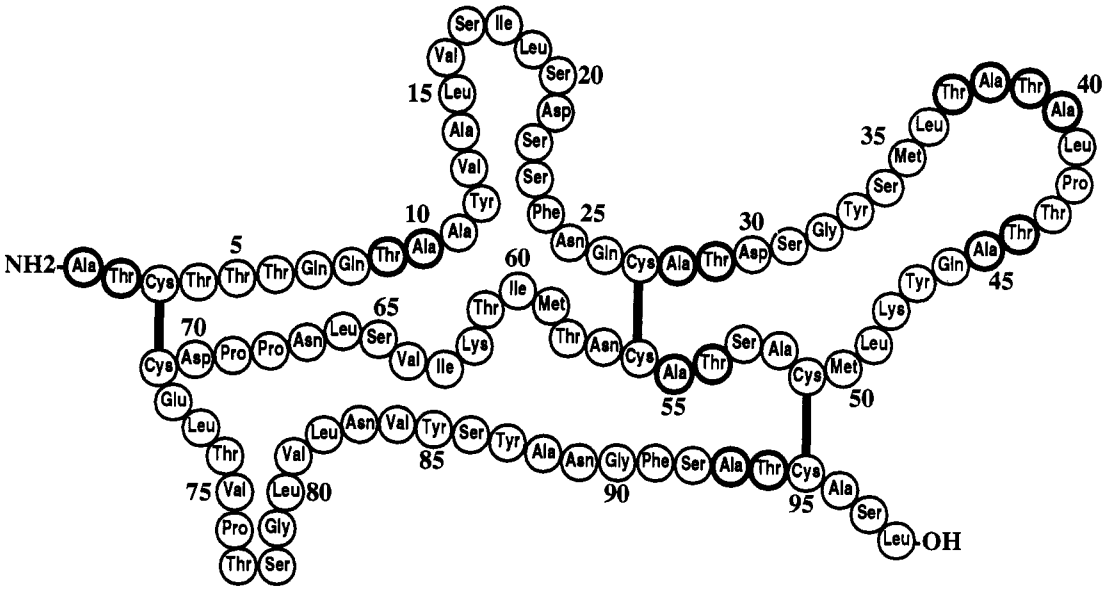

FIGURE 1: Primary structure of capsicein showing the three disulfide bridges, 3–71, 27–56, and 51–95, and the high frequency of Ala-Thr and Thr-Ala pairs. One-third of the sequence is made up of 16 threonines, 13 alanines, and 12 serines.

Zuiderweg, 1988; Marion et al., 1989a) and clean-TOCSY-HMQC experiments (Marion et al., 1989b) were performed on uniformly ^{15}N-labeled capsicein. 3D HMQC-NOESY-HMQC (Ikura et al., 1990; Frenkiel et al., 1990) proved extremely powerful in the case of this highly helical protein, far beyond its usual application of solving ^{1}H degeneracies. Assignments given in this paper cover all proton and nitrogen nuclei. All secondary structures of capsicein were identified, allowing a preliminary reconstruction of its three-dimensional structure.

MATERIALS AND METHODS

Protein Enrichment and Purification. *Phytophthora capsici* Leonian, isolate A147, derived from pepper (*Capsicum annuum*) was obtained from the culture collection at INRA Antibes. It was grown in Roux bottles in a liquid medium as described (Pernollet et al., 1993) with 5 g L^{-1} $K^{15}NO_3$ (98.9% ^{15}N labeling) as the only nitrogen source. After 15 days of culture in darkness at 26 °C, culture filtrates were filtered through 0.22-μm filters. Labeled capsicein was purified by RPLC as described (Nespoulous et al., 1992; Huet et al., 1992; Huet & Pernollet, 1993). Labeled elicitin fractions were lyophilized before use. Twenty milligrams of capsicein was dissolved in a mixture of 90% H_2O/10% D_2O. The concentration of the sample was about 4 mM, and the uncorrected pH was 6.85, unless specified.

Homonuclear NMR Spectroscopy. 2D DQF-COSY (Aue et al., 1976), HOHAHA (Braunschweiler & Ernst, 1983), and NOESY (Jeener et al., 1979) were performed on a Bruker AM600 spectrometer equipped with an Aspect 3000 computer. All spectra were recorded in pure phase absorption using time proportional phase increments (Redfield & Kuntz, 1975), with a spectral width of 11.73 ppm, at 45 °C and pH 6.85. All data sets were collected as 512 and 2048 points in the t_1 and t_2 dimensions, respectively. For NOESY two mixing times of 150 and 200 ms were used, and for HOHAHA three MLEV-17 mixing sequences of 40, 60, and 80 ms were used. Clean-TOCSY was employed to compensate for the ROESY contribution. A technique known as SCUBA (stimulated cross peaks under bleached alphas) was used to recover magnetization of α-protons which were saturated by irradiation of solvent (Brown et al., 1988). Measurement of the coupling constant ^{3}JNHα was carried out following the method proposed by Ludvigsen (Ludvigsen et al., 1991). This technique allows an accurate measurement of these values by addition and subtraction of the traces from NOESY and COSY experiments after scaling. The method was adapted in the GIFA software[2] with an automated evaluation of the scaling factor based on the symmetry of the resulting peak after subtraction or addition. It is shown to give accurate measurements of the coupling constants. Because of the high degree of overlap in 2D experiments, only two-thirds of the ^{3}JNHα values were measured, and these have confirmed the secondary structures established. For residues involved in β-sheets, values of about 10 Hz were found, and for residues contained in α-helices, values from 4 to 7 Hz were measured. The values of these different constants were used to calculate dihedral angles from the Karplus equation (Karplus, 1959; Bystrov, 1976; Pardi et al., 1984).

Heteronuclear NMR Spectroscopy. 2D HMQC, 2D HSQC, 2D HMQC-NOESY, and 3D HMQC-NOESY-HMQC were performed on a Bruker AMX600 on the ^{15}N-labeled sample; all other heteronuclear experiments were performed on a Bruker AM400 spectrometer equipped with an Aspect 3000 computer. All spectra were recorded at 45 °C. 2D HMQC (Mueller, 1979; Bax et al., 1983; Sklenár & Bax, 1987) and 2D HMQC-NOESY experiments (Gronenborn et al., 1989) were recorded with 512 t_1 points and 2048 t_2 points. The spectral width was set to 7042.25 Hz in the F_2 dimension and 2885 Hz in the F_1 dimension. The ^{1}H carrier was set at 4.8 ppm, and the ^{15}N chemical shifts are relative to NH_4Cl (1 M in 1 M HCl). Suppression of the solvent resonance was achieved by presaturation during the 1-s relaxation delay and during the 150-ms mixing time in the HMQC-NOESY experiment. Broad-band decoupling with the GARP sequence (Shaka et al., 1985) was used during the acquisition period. 3D NOESY-HMQC (Fesik & Zuiderweg, 1988; Marion et al., 1989a) and 3D clean-TOCSY-HMQC experiments (Marion et al., 1989b) were used. In both 3D experiments, presaturation of the solvent signal was performed by low-power irradiation during the relaxation delay to

[2] The GIFA NMR software (M. A. Delsuc, 1992) used throughout this work has been developed in this laboratory and is available from the authors.

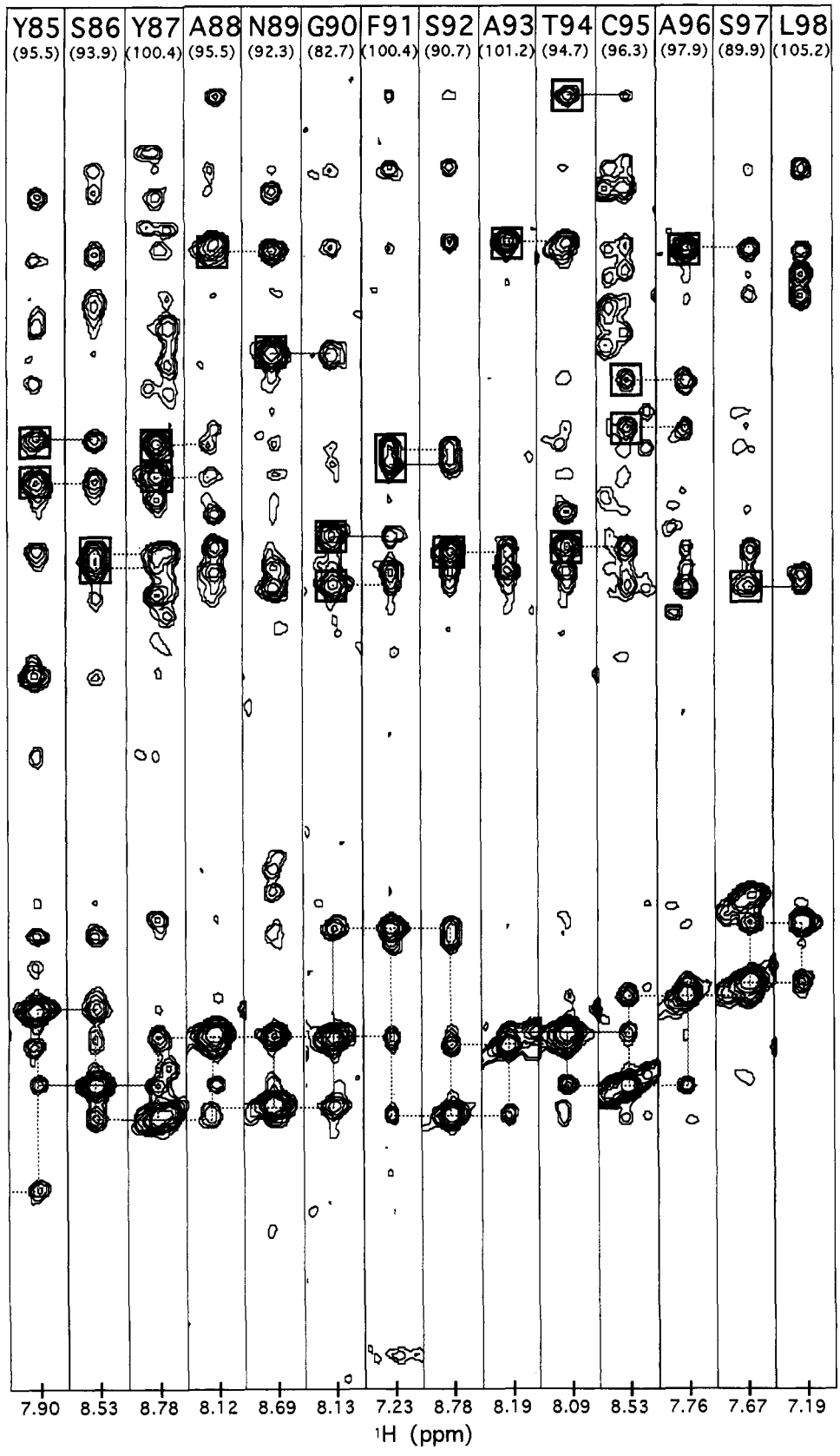

FIGURE 2: (ω_1, ω_3) slices of the 3D NOESY-HMQC spectrum of the uniformly ^{15}N-labeled capsicein protein. Each slice is taken at the amide nitrogen frequency of residues Tyr 85 to Leu 98 and shows all of the C-terminal α-helix. dNN(i, i–1) and dNβ(i, i–1) NOESY cross peaks are joined by dashed lines. The diagonal peak and cross peak to the preceding residue and the next residue are connected. Residue number and ^{15}N and amide proton chemical shifts are indicated for each slice. Intraresidual cross peaks are boxed.

eliminate the H_2O resonance. Spectral widths were set to 5000, 1923, and 5000 Hz, and a matrix of 256, 64, and 1024 points in the F_1, F_2, and F_3 dimensions, respectively, was acquired. TPPI was used in the t_1 and t_2 time domains to discriminate the frequency signs. The spectra were recorded as a series of two-dimensional homonuclear experiments incrementing the t_2 delay. Finally, a 3D HMQC-NOESY-HMQC experiment (Ikura et al., 1990; Frenkiel et al., 1990)

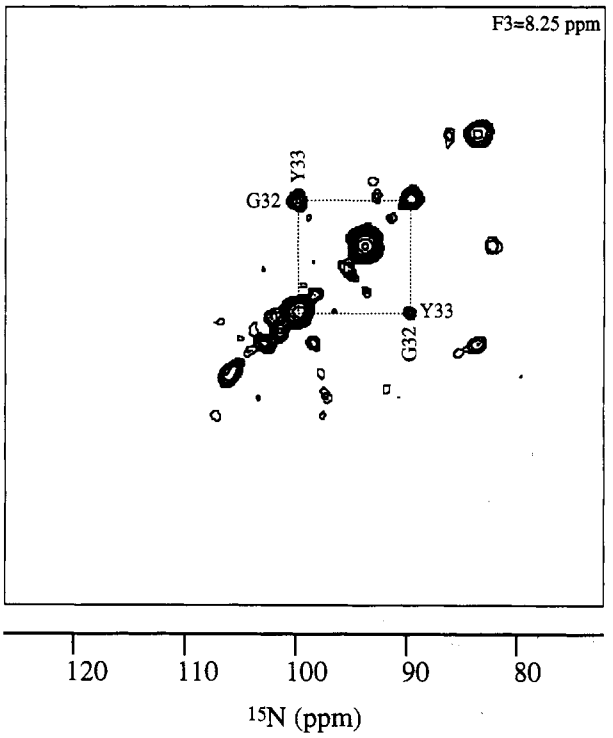

FIGURE 3: (ω_1, ω_2) slices of the HMQC-NOESY-HMQC spectrum at 600 MHz of uniformly ^{15}N-labeled capsicein, in H_2O at pH 6.85 and 45 °C. The coordinates along both dimensions are those of the nitrogens linked to the spatially close amide protons. The extracted plane is perpendicular to the proton frequency axis. Two residues (Gly 32 and Tyr 33), involved in an α-helical structure and whose amide protons have the same chemical shift, are shown to have spatially close amide protons. The dNN(32, 33) correlation cannot be observed in any other experiment.

was performed on an AMX600 spectrometer equipped with an X32 computer using the same experimental conditions. All spectra were Fourier transformed and processed on a RISC 6000 IBM computer with the GIFA and GIFC NMR software developed in our laboratory (M. A. Delsuc). A 3D matrix of 256 × 128 × 512 points in the ω_1, ω_2, and ω_3 dimensions, respectively, was obtained after zero filling and Fourier transformation.

RESULTS AND DISCUSSION

Assignment Procedure. Two methods were employed to identify the residues and assign all the proton and nitrogen resonances of the protein.

The first strategy was based on the use of the HMQC spectra. Each correlation between a nitrogen-15 and its attached amide proton was defined by a pair of coordinates, (ω_1, ω_2), corresponding to the ^{15}N and proton chemical shifts in the F_1 and F_2 dimensions, respectively. ω_1 traces at the (ω_2, ω_3) frequency were extracted from the three-dimensional NOESY-HMQC and TOCSY-HMQC experiments and compared. A trace extracted from the 3D TOCSY-HMQC spectra allows the identification of the spin systems, and a trace from the 3D NOESY-HMQC permits the identification of the protons close to the amide proton. Differences between the TOCSY line and the NOESY line correspond to protons of other spin systems seen by this amide proton. The goal is then to identify all of the spin systems and classify them by common correlations existing between all lines.

The second strategy consisted in extracting planes perpendicular to the ^{15}N frequency in the 3D TOCSY-HMQC and 3D NOESY-HMQC experiments. The planes obtained could be compared to the results of 2D NOESY and HOHAHA experiments. Yet as these planes were ^{15}N-edited, the signal present in each plane was drastically reduced. To perform the assignment, ω_1 lines along the amide proton frequency were compared, thus identifying individual spin systems.

Our assignment was first based on the recognition of specific patterns of secondary structures followed by their positioning in the primary sequence from some specific assignments of residues. This is merely an extension of the main chain directed method proposed by Wand (Englander & Wand, 1987; Wand & Nelson, 1988). Advantage is taken from the increased legibility of the 3D data sets. The identification of residues and their assignment are carried out at the same time as the secondary structure classification. The rest of the assignment proceeds as proposed by Wüthrich (Wüthrich, 1986) and consists in the identification of all remaining spin systems from the ω_1 lines from 3D TOCSY-HMQC and the identification of the sequential connections from the ω_1 lines extracted from 3D NOESY-HMQC.

Spin System Classification. One-third of capsicein is composed of 16 threonines, 13 alanines, and 12 serines, with 9 different possible Thr-Ala or Ala-Thr pairs, which made the assignment very difficult. Threonines were distinguished from alanines by their Hα-Hβ correlation on DQF-COSY,

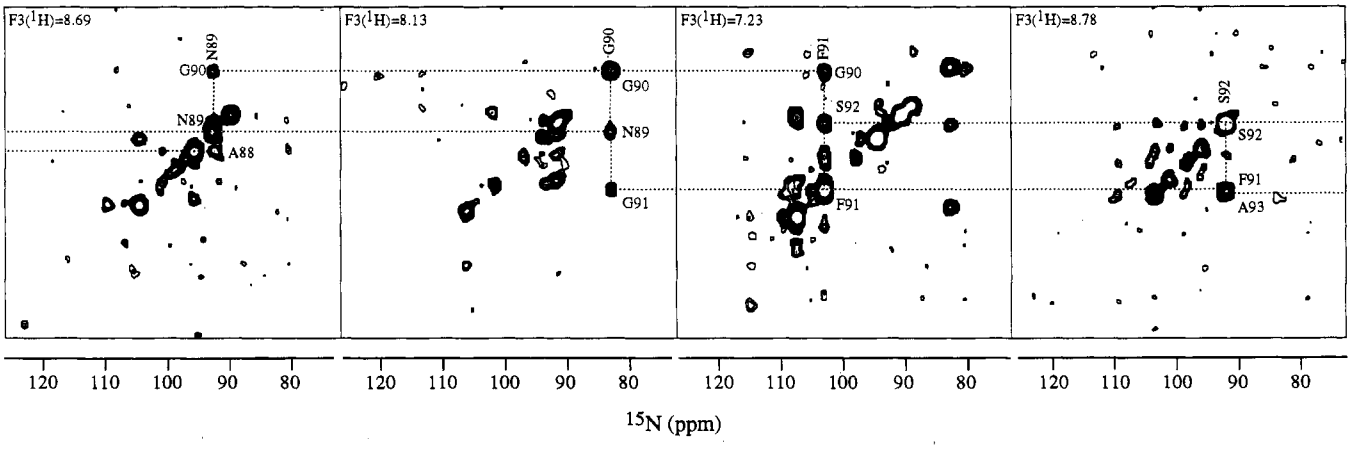

FIGURE 4: (ω_1, ω_2) slices of the HMQC-NOESY-HMQC spectrum at 600 MHz of uniformly ^{15}N-labeled capsicein, in H_2O at pH 6.85 and 45 °C. The four planes are chosen perpendicular to the amide proton frequency and show how the determination of the residues involved in helical structure is greatly facilitated. Residues Asn 89 to Ser 92 involved in the C-terminal α-helix are shown. The two dimensions of the planes show the ^{15}N chemical shift, and the cross peaks between two nitrogens along the F_1 dimension indicate a spatial proximity between the two amide protons linked to the nitrogens. Dashed lines join dNN(i, i+1) and dNN(i, i–1) cross peaks. Each peak on the diagonal has two cross-peak correlations, as expected in an α-helix. The NOESY walk is made from one plane to the next.

but the overlap was so great that the identification and assignment were not made with great confidence and were confirmed from the 3D experiments. The three glycines were easily identified on the HMQC experiment, as the ^{15}N chemical shifts of these residues are at high field and each shows a pair of NH–Hα correlations on the corresponding TOCSY-HMQC planes; they were further confirmed on 2D DQF-COSY by their large coupling constant and on a 2D TQF-COSYspectrum. Aromatic protons were identified on DQF-COSY in D_2O, and their amide proton was found by the correlation between CδH_2 and CβH_2 on the NOESY spectra. In the case of an overlap with amide protons, the ambiguities in the NOESY spectrum can be solved by inspection of the NOESY-HMQC, where the only correlations to be found refer to the amide protons. Thus, five tyrosines and two phenylalanines were found. The TOCSY-HMQC spectrum allowed the identification of the NH_2 side chains of asparagines and glutamines, since they show, on the corresponding (ω_1, ω_3) slice, a pair of symmetrical cross peaks in the high-field region. The glutamines were distinguished from the asparagines on the basis of the length of the side chain. Three of the four prolines were detected on the NOESY spectra and cannot be seen on the HMQC spectra since no proton is directly linked to the nitrogen. Valines were recognized by the characteristic chemical shift of the α-proton at high field. AMX systems were assigned on the basis of adjacent residues. All the assignments of overlapping spin systems have been made possible with 3D NOESY-HMQC, TOCSY-HMQC, and HMQC-NOESY-HMQC as discussed below.

Assignment of α-Helical Regions. Residues involved in α-helical structures were rapidly identified by strong NH(i)–NH(i+1) NOEs, weak NH(i)–Hα(i–1) NOEs, medium or strong NH(i)–Hβ(i–1) NOEs, and very weak intraresidue NH–Hα correlations in 3D TOCSY-HMQC spectra because of the small coupling constant for this type of structure. The following technique was applied. A dNN cross peak was located between two amide protons in an (ω_1, ω_3) NOE plane. The symmetrical correlation exists in another plane, allowing two adjacent residues to be identified. They can be ordered through the sequential dNα(i, i–1) and dNβ(i, i–1) correlations. When several residues are shown to be in an α-helical structure, other important correlations such as dNα(i, i–3) and dNN(i, i+3) can be identified. Figure 2 shows an example of this assignment procedure for the α-helical region, from tyrosine 85 to C-terminal extremity leucine 98. Each slice of the ^1H–^{15}N NOESY-HMQC spectrum is taken at the nitrogen frequency; a sequential NH(i)–NH(i–1) NOESY walk is indicated by dashed lines, as are sequential Hβ(i–1)–HN(i) connections. For each (ω_1, ω_3) slice taken at the ω_2 frequency, a portion of the amide proton considered is extracted. Comparison between slices from 3D NOESY-HMQC and TOCSY-HMQC spectra allows inter- and intraresidue correlations to be distinguished. Each amide proton is linked to two different amide protons in adjacent panels by dashed lines, as are HN(i) correlations with Hβ(i–1) of the preceding residue. This method led to the assignment of the residues in five helical regions located from Thr 5 to Ile 18, from Gln 26 to Tyr 33, from Thr 44 to Thr 58, from Met 59 to Asn 67, and from Ser 86 to Leu 98, equivalent to more than 60% of the residues in the protein, in agreement with circular dichroism studies (Nespoulous et al., 1992).

3D HMQC-NOESY-HMQC. In the case of α-helices, amide protons resonate within a very narrow chemical-shift range, and a great deal of overlap may occur as the size of the protein increases. The 3D NOESY-HMQC experiment alleviates many of these problems by spreading information along the heteroatom axis. Thus assignments of residues involved in α-helical structures are easily made by identifica-

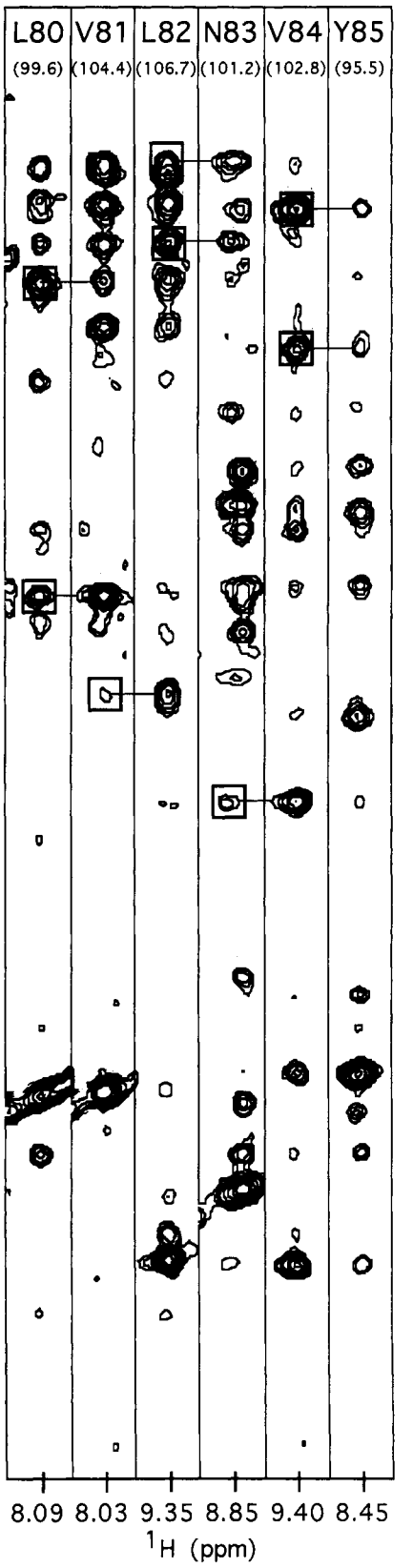

FIGURE 5: (ω_1, ω_3) slices of the 3D NOESY-HMQC spectrum of uniformly ^{15}N-labeled capsicein. Panels correspond to residues Leu 80 to Tyr 85 involved in a β-sheet. Slices are taken at the backbone amide nitrogen frequency of residues 80–85. NOESY connectivities dNα(i, i–1) and dNβ(i, i–1) are joined by dashed lines. Residue number and ^{15}N and amide proton chemical shifts are indicated on each slice. Intraresidual cross peaks are boxed.

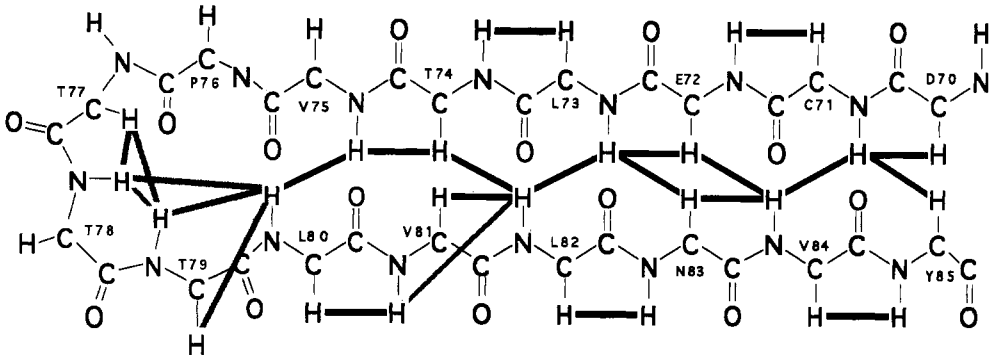

FIGURE 6: Schematic representation of the topology of the β-sheet found in capsicein. Residues Asp 70 to Val 75 and Leu 80 to Tyr 85 make two strands of six residues forming the β-sheet. The two strands are linked by a β-turn of four residues, Pro 76 to Gly 79. Thick lines indicate inter- or intrastrand NOESY connections, and dashed lines indicate other NOESY connections within the β-turn, as found from NOESY-HMQC.

tion of NH(i)–N(i+1)–NH(i+1) correlations. This method is successful as long as the ^{15}N and the amide proton do not have the same or similar chemical shifts. ^{15}N degeneracies would lead to dNN correlations appearing in one single plane of the NOESY-HMQC experiment. In the present case, the corresponding planes from the 3D TOCSY-HMQC all showed analogous dNN cross peaks, clearly identifying them as the geminal protons of asparagine or glutamine side chains. If, on the other hand, the amide proton resonances are almost degenerate, the NH(i)–N(i+1)–NH(i+1) cross peak is greatly perturbed by the diagonal peak NH(i)–N(i)–NH(i). In this case, the usual 3D NOESY-HMQC cannot resolve this indetermination. A possible solution to assign these residues is to perform 3D HMQC-NOESY-HMQC (Ikura et al., 1990; Frenkiel et al., 1990). In this experiment, along two of the three frequency axes we observe the nitrogen-15 chemical shift, and instead of observing a cross peak between NH(i) and NH(i+1), we look for cross peaks between N(i) and N(i+1). It now becomes possible to demonstrate that residues (i) and (i+1) are successive in a helix even if both amide protons have the same chemical shift, because the HMQC-NOESY-HMQC correlates nitrogens whose amide protons are close through space, and not protons. Figure 3 illustrates one (ω_1, ω_2) plane perpendicular to the ω_3 axis taken at the amide proton frequency δ = 8.25 ppm. At this chemical shift we find two amide protons corresponding to glycine 32 and tyrosine 33 which are involved in an α-helix. Thus, in the (ω_1, ω_2) cross plane, in addition to the two diagonal peaks corresponding to G32 and Y33, we observe two cross correlations between the two frequencies. The assignment of these two residues remained tentative until this experiment was performed. Other such pairs are Thr 58-Met 59 and Ile 63-Val 64. The spreading of the information along the heteroatom axis may be used to resolve these difficult cases, but it is also extremely useful in the case of two residues in an α-helical structure. As such, HMQC-NOESY-HMQC may probably be considered as the fastest method to determine the frequency of the amide protons involved in α-helices since only NH–NH correlations need to be characterized. Figure 4 shows this application in the α-helical segment from asparagine 89 to serine 92. Slices represented are (ω_1, ω_2) planes extracted perpendicular to the ω_3 axis at the amide proton frequency of each residue. F_1 and F_2 coordinates are those of ^{15}N heteroatoms. Proceeding along ω_1, indicated by dashed lines connecting N(i)–N(i+1) and N(i)–N(i–1), may be considered as an equivalent of the so-called NOESY walk. In this case, amide protons do not have the same chemical shift and no cross peak appears between two diagonal peaks in the same (ω_1, ω_2) plane.

Assignment of a β-Sheet. Distances between amide protons in β-sheets are shorter than those encountered in α-helical structures. Conversely, residues involved in β-sheets show strong intraresidual dNα correlations in TOCSY spectra and weak intraresidual dNα and very strong interresidual dNα(i, i–1) correlations in NOESY spectra. If the dNN(i, i–1) correlation is detected, it is very weak. Figure 5 shows panels extracted from (ω_1, ω_3) slices perpendicular to the nitrogen axis at the amide proton frequency of the 3D NOESY-HMQC experiment. Residues Leu 80 to Tyr 85 are represented. Each amide proton has a dNα(i, i–1) or dNβ(i, i–1) connection with the preceding residue. This is an example of the assignment of one strand of a β-sheet, and this method is equally efficient for residues in extended regions. A double-stranded β-sheet was located involving residues Asp 70 to Val 75 for one strand and continuing from Leu 80 to Tyr 85 for the other one. Figure 6 shows the schematic representation of the topology of the β-sheet. The two strands are linked by a turn from residue Pro 76 to Gly 79. Interstrand or intrastrand correlations are indicated by thick lines, and the dashed lines indicate connections within the turn. In reverse experiments the interstrand dαα(i, j) correlations are not observable, but dNN(i, j) or dNα(i, j) correlations are seen. The β-sheet-specific dαα(i, j) connections had to be looked for on the 2D homonuclear spectra.

Other Conformations: Extended Regions and Turns. Regions making up turns are located from Pro 76 to Gly 79 and from Ala 40 to Thr 43. The 76–79 turn links the two strands of the β-sheet (Figure 6). In this turn, serine 78 seems to have an important role and its hydroxyl proton is involved in a hydrogen bond. This proton is seen in the NOESY spectra as well as in the HOHAHA spectra, where it shows correlations to the whole spin system of the serine, demonstrating a slow exchange with the water protons. Proximity is clearly established between Ser 78, Val 75, and Leu 80. Assignment of extended structures is carried out by searching for strong dNα(i, i–1) NOEs. dNN connections do not appear, as compared to those found for residues facing each other in β-sheet structures.

Solvent Accessibility. A rapid exchange of the amide protons with the water protons at high pH (6.85) revealed the exposure of several residues to the solvent. The spin systems whose amide protons are very rapidly exchanged are not visible in the spectra. Therefore experiments at pH 5.35, where the exchange is slowed, were performed. In particular, reverse HMQC, NOESY, and TOCSY experiments allowed the assignment of these residues. Comparison of HMQC spectra at pH 6.85 and 5.35 showed six residues (Thr 5, Ser 22, Ser 23, Thr 43, Thr 44, and Thr 54) that appear only in the low-

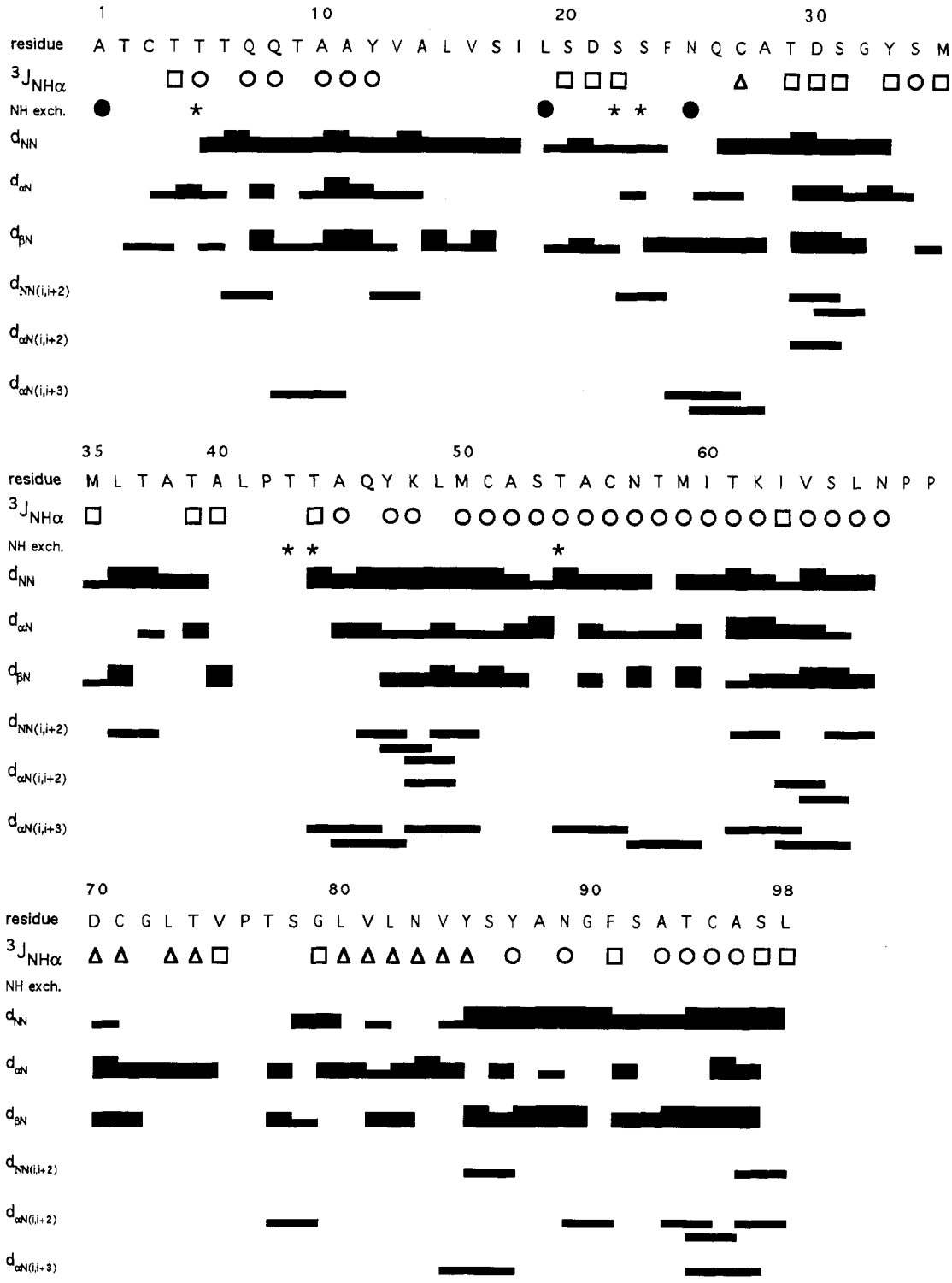

FIGURE 7: Summary of sequential assignment of capsicein. A bar between two residues attests that a connectivity [dNN, dNα(i, i–1), dNβ(i, i–1), etc.] has been observed between these two residues. Wide, medium and narrow bars indicate respectively strong, medium, and weak NOESY intensities. Open circles, squares, and triangles indicate coupling constants smaller than 6 Hz, coupling constants between 6 and 9 Hz, and coupling constants greater than 9 Hz, respectively. Stars and filled circles indicate amide protons observable at lower pH only or amide protons not detected even at low pH in the 2D reverse experiments, respectively.

pH spectrum. Ala 1, Leu 19, and Asn 25 are not detected on the 2D reverse experiments even at low pH. Most of these residues are located in the loops, in particular in the Leu 19 to Asn 25 region.

Global Fold Analysis. A combination of 2D homonuclear and heteronuclear experiments with 3D reverse experiments was necessary for the assignment (Table 1). A summary of the sequential resonance assignment and the relative intensities of cross peaks used is presented in Figure 7. An evaluation of the coupling constant has been given whenever the measurement was possible. One should note that the efficiency of the NH–Hα HOHAHA transfer as seen from 3D TOCSY-HMQC gives a clear evaluation of the corresponding coupling as seen from the poor transfer in the helical regions compared to that in the extended regions. Five helical regions and a short antiparallel β-sheet are observed in the global three-dimensional fold of capsicein. Each strand of the β-sheet contains six residues linked by a β-turn. This last arrangement

Table 1: Capsicein ^1H and ^{15}N Chemical Shifts (45 °C, pH 6.85)

residue	^{15}N	HN	Hα	Hβ	others
A1					
T2	89.1	8.71	4.68	4.31	$C^{\gamma}H_3$ 1.57
C3	102.0	8.99	5.05	3.77, 2.89	
T4	93.9	9.36	4.71	4.90	$C^{\gamma}H_3$ 1.59
T5	95.5	9.11	4.32	3.76	$C^{\gamma}H_3$ 1.52
T6	97.1	8.12	4.30	4.43	$C^{\gamma}H_3$ 1.47
Q7	99.6	7.65	4.30	2.48, 2.22	$C^{\gamma}H_2$ 2.68; $N^{\epsilon}H_2$ 7.76, 6.92; N^{ϵ} 88.3
Q8	96.3	9.05	3.76	2.51, 2.33	$C^{\gamma}H_2$ 2.86, 2.70; $N^{\epsilon}H_2$ 7.78, 7.14; N^{ϵ} 89.1
T9	90.7	7.92	4.44	4.04	$C^{\gamma}H_3$ 1.82
A10	98.7	7.49	4.29	1.71	
A11	98.7	8.71	4.11	1.56	
Y12	93.9	8.80	4.52	3.27, 3.10	$C^{\delta}H$ 7.19; $C^{\epsilon}H$ 6.88
V13	97.1	8.53	3.50	2.32	$C^{\gamma}H_3$ 1.11
A14	99.6	7.82	4.30	1.68	
L15	93.9	8.53	4.14	1.62, 2.15	$C^{\gamma}H$ 2.05; $C^{\delta}H_3$ 0.97
V16	93.9	8.78	3.56	2.29	$C^{\gamma}H_3$ 1.15, 1.02
S17	90.7	7.87	4.30	4.02, 3.55	
I18	104.4	8.18	4.60	2.79	$C^{\gamma}H_3$ 2.06; $C^{\delta}H_3$ 0.97
L19		8.05	3.74	1.77, 1.63	$C^{\gamma}H$ 1.28; $C^{\delta}H_3$ 0.69, 0.25
S20	86.7	7.45	4.49	4.21, 4.01	
D21	101.2	7.88	5.02	3.19, 2.86	
S22	100.4	9.63	4.22	4.29	
S23	93.1	9.09	4.63	4.35, 4.25	
F24	101.2	7.97	4.46	3.59, 3.50	$C^{\delta}H$ 7.51, $C^{\epsilon}H$ 7.38
N25		8.73	4.62	3.13, 3.08	$N^{\delta}H_2$ 7.22, 7.09; N^{δ} 87.5
Q26	96.3	8.14	4.18	2.04	$C^{\gamma}H_2$ 2.58, 2.38; $N^{\epsilon}H_2$ 8.20, 7.09; N^{ϵ} 93.1
C27	94.7	8.72	4.65	3.31, 3.06	
A28	102.0	8.07	4.46	1.45	
T29	93.9	8.28	4.15	4.47	$C^{\delta}H_3$ 1.45
D30	98.7	8.98	4.56	3.11, 2.91	
S31	86.7	8.41	4.51	4.18, 4.01	
G32	89.1	8.20	4.39, 4.02		
Y33	98.7	8.27	4.62	3.14, 2.45	$C^{\delta}H$ 7.09; $C^{\epsilon}H$ 6.79
S34	97.9	7.85	4.76	3.91, 3.74	
M35	102.8	8.55	4.00	2.24, 2.13	$C^{\gamma}H_2$ 2.62, 2.69; $C^{\delta}H_3$ 1.99
L36	90.7	7.95	4.46	1.81, 1.86	$C^{\delta}H_3$ 1.27, 1.02
T37	81.9	7.37	4.22	4.49	$C^{\gamma}H_3$ 1.27
A38	103.6	7.84	4.44	1.49	
T39	83.5	8.27	4.46	4.77	$C^{\gamma}H_3$ 1.50
A40	101.2	8.02	4.83	1.72	
L41	97.9	8.48	4.67	2.04, 2.08	$C^{\gamma}H$ 1.94; $C^{\delta}H_3$ 1.30, 1.24
P42			4.32	1.12, 0.83	$C^{\gamma}H_2$ 1.31, 0.24; $C^{\delta}H_2$ 3.68, 3.58
T43	95.5	9.00	4.28	4.43	$C^{\gamma}H_3$ 1.59
T44	93.9	9.02	4.25	4.37	$C^{\gamma}H_3$ 1.50
A45	99.6	8.26	4.22	1.60	
Q46	93.9	7.80	4.28	2.75, 2.47	$C^{\gamma}H_2$ 3.15, 2.98; $N^{\delta}H_2$ 7.49, 7.24; N^{ϵ} 87.
Y47	97.9	9.28	4.45	3.16, 3.06	$C^{\delta}H$ 7.12, $C^{\epsilon}H$ 6.88
K48	95.5	8.61	4.00	2.46, 2.12	$C^{\gamma}H_2$ 1.91, 1.87; $C^{\delta}H_2$ 1.63; $C^{\epsilon}H_2$ 3.66
L49	93.9	7.34	4.35	2.27, 1.68	$C^{\delta}H_3$ 1.25, 1.14
M50	96.3	8.90	4.43	2.75, 2.45	$C^{\gamma}H_2$ 3.12, 2.96; $C^{\delta}H_3$ 2.02
C51	93.1	9.46	4.37	3.05	
A52	96.3	7.18	4.60	1.67	
S53	91.3	7.49	5.06	4.35, 4.23	
T54	107.4	9.56	4.75	4.43	$C^{\gamma}H_3$ 1.53
A55	102.8	8.67	4.44	1.66	
C56	93.1	9.02	4.69	3.09, 3.03	
N57	95.5	8.45	4.46	3.26, 2.95	$N^{\delta}H_2$ 7.73, 7.04; N^{δ} 90.7
T58	96.3	8.80	4.11	4.62	$C^{\gamma}H_3$ 1.47
M59	100.4	8.74	4.10	2.55, 2.26	$C^{\gamma}H_2$ 2.61, 2.85; $C^{\delta}H_3$ 2.36
I60	96.3	8.37	3.78	2.03	$C^{\gamma}H_2$ 1.34, 0.96; $C^{\gamma}H_3$ 0.39; $C^{\gamma}H_3$ –0.07
T61	93.1	8.17	4.07	4.55	$C^{\gamma}H_3$ 1.51
K62	99.6	8.35	4.28	2.21, 2.10	$C^{\gamma}H_2$ 1.59; $C^{\delta}H_2$ 1.80, 1.72; $C^{\epsilon}H_2$ 3.06
I63	97.1	8.59	3.73	2.32	$C^{\delta}H_3$ 1.09
V64	95.5	8.63	3.65	2.43	$C^{\gamma}H_3$ 1.14, 0.98
S65	92.3	7.99	4.57	4.29, 4.10	
L66	99.6	7.88	4.48	2.18, 2.10	$C^{\gamma}H$ 1.80; $C^{\delta}H_2$ 1.18, 1.07
N67	90.7	8.16	4.89	3.29, 2.94	$N^{\delta}H_2$ 7.68, 6.97; N^{δ} 89.9
P68					
P69				2.12, 2.22	$C^{\gamma}H_2$ 1.97; $C^{\delta}H_2$ 4.18, 4.10
D70	97.9	8.36	5.14	2.73, 1.71	
C71	94.7	7.91	5.00	3.53, 3.19	
E72	95.5	8.59	4.50		
L73	106.7	9.14	4.83	2.07, 1.80	$C^{\delta}H_3$ 0.89
T74	96.3	8.53	4.99	4.12	$C^{\gamma}H_3$ 1.12
V75	110.0	9.77	4.13	2.53	$C^{\gamma}H_3$ 1.24, 1.11
P76					
T77	82.6	7.36	4.22	4.52	$C^{\gamma}H_3$ 1.27

Table 1: (Continued)

residue	^{15}N	HN	Hα	Hβ	others
S78	90.7	7.53	4.72	3.69, 3.48	OH 6.12
G79	89.1	8.52	4.38, 3.67		
L80	99.6	8.09	4.17	1.78, 1.49	$C^{\delta}H_3$ 0.96, 0.85
V81	104.4	8.03	4.96	2.12	$C^{\gamma}H_3$ 1.18, 0.93
L82	106.7	9.35	4.86	1.72, 1.47	$C^{\delta}H_3$ 0.96, 0.85
N83	101.2	8.85	5.78	3.50, 2.78	$N^{\delta}H_2$ 8.21, 7.54; N^{δ} 89.9
V84	102.8	9.40	3.69	2.30	$C^{\gamma}H_3$ 1.18, 0.83
Y85	95.5	7.90	4.44	3.25, 2.95	$C^{\delta}H$ 7.31; $C^{\epsilon}H$ 7.04
S86	93.9	8.53	4.20	4.28, 4.24	
Y87	100.4	8.78	4.48	3.53, 3.23	$C^{\delta}H$ 7.16; $C^{\epsilon}H$ 6.78
A88	95.5	8.12	4.27	1.62	
N89	92.3	8.69	4.43	2.53, 2.45	$N^{\delta}H_2$ 6.92, 6.75; N^{δ} 89.9
G90	82.7	8.13	4.38, 3.99		
F91	100.4	7.23	4.31	3.40, 3.28	$C^{\delta}H$ 7.44; $C^{\epsilon}H$ 7.34; $C^{\zeta}H$ 7.09
S92	90.7	8.78	4.10	3.37, 3.24	
A93	101.2	8.19	4.29	1.56	
T94	94.7	8.09	3.80	4.05	$C^{\gamma}H_3$ 0.33
C95	96.3	8.53	4.40	2.72, 2.31	
A96	97.9	7.76	4.41	1.62	
S97	89.9	7.67	4.78	4.16, 4.10	
L98	105.2	7.19	4.31	2.03, 1.87	$C^{\gamma}H$ 1.68; $C^{\delta}H_3$ 1.02, 0.94

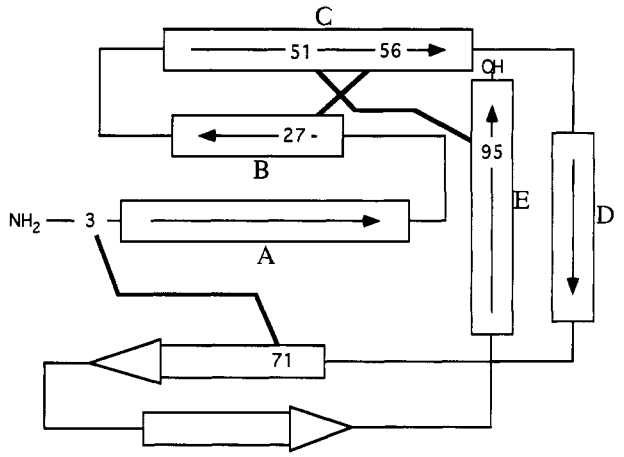

FIGURE 8: Schematic representation of capsicein showing five α-helical structures and one antiparallel β-sheet. Four of the helices comprise two pairs running antiparallel, while the last one is parallel to the β-sheet. Three disulfide bridges connect these different secondary structures, allowing the global tertiary fold of capsicein.

is known as a β-wing. The helices extend from Thr 5 to Ile 18, from Glu 26 to Tyr 33, from Thr 44 to Thr 58, from Met 59 to Asn 67, and from Ser 86 to Leu 98. They are respectively called A, B, C, D, and E. Helices C and D are contiguous and could be described as a bent helical fragment. A large proportion of α-helix was already shown in capsicein through circular dichroism. NOESY cross peaks were observed between residues in helices B and C and those in helices D and E, showing that these helices are close in space. Four of the five helices can be grouped in two antiparallel pairs (A and B, D and E), and the fifth one runs parallel to the β-sheet (Figure 8). This fold is due in part to the location of the disulfide bridges that connect the secondary structures. Chemical methods have only identified one disulfide bridge, that between Cys 3 and Cys 71, and the two other were identified by proximities existing between Cys 51 and Cys 95 and between Cys 27 and Cys 56. The first three-dimensional reconstructions by distance-geometry computations support these assignments and will be reported later. Loops connecting the helices seem less structured, particularly the Leu 19 to Asn 25 and Ala 40 to Thr 44 regions, as shown by increased solvent accessibility in these regions. In addition, NOESY cross peaks are observed between Tyr 12, Tyr 85, and Tyr 87 and between Tyr 47 and Phe 91, indicating that they are in close proximity, forming an aromatic cluster around which the secondary structures are packed.

CONCLUDING REMARKS

It is shown here that 3D heteronuclear NMR is an efficient tool to assign all of the proton and ^{15}N resonances in capsicein, a member of a protein family for which no prior structural knowledge from X-ray data is available, with the aim of its three-dimensional structure reconstruction. Contrarily to homonuclear experiments, heteronuclear experiments need special treatment of the protein to incorporate NMR-sensitive nuclei such as ^{15}N or ^{13}C. Advantage was taken in the present study of the easy incorporation of the ^{15}N label by growing the fungus on $K^{15}NO_3$ as the sole source of nitrogen. Residues are unambiguously identified by 3D TOCSY-HMQC, and secondary structures (α-helices, turns, β-sheets, extended structures, and loops) are easily identified by 3D NOESY-HMQC. All overlaps are suppressed by spreading the information along the ^{15}N axis. In particular, 3D HMQC-NOESY-HMQC allows the assignment of residues with degenerate amide resonances. But in addition, we showed how this experiment simplified the assignment in the case of α-helical structures. More than 1000 distance constraints were obtained from the analysis of the 2D and 3D NOESY experiments, and over 60 angle constraints were obtained from the DQF-COSY experiment. These NMR-determined distances and torsion angles provide a good starting point for the calculation of the three-dimensional structure of capsicein. This work is underway and will be presented in the near future.

At first sight, the C-terminal secondary structure motifs of capsicein evoke phospholipase structural features, *i.e.* a β-wing linking two α-helices (Scott & Sigler, 1994). Despite the absence of sequence homology between these enzymes and elicitins, this hypothesis is supported by results stating that a β elicitin directly interacts with and disturbs the plasma membrane of cultured tobacco cells (Blein et al., 1991). If elicitins were able to release fatty acids from the lipids of the plasma membrane due to some phospholipase activity, their mode of action could be directly related to the jasmonic acid defense signaling pathway occurring *in vivo*, a mechanism known to act in plant cells for the specific expression of defense genes (Farmer & Ryan, 1992; Sembdner & Parthier, 1993). The knowledge of the three-dimensional structure of capsicein

will help in the elucidation of the three-dimensional structures of other homologous proteins, and most interestingly of basic elicitins, whose biological activity is differentiated mainly by residue 13. Insight into the structure–activity of this novel class of proteins will then probably be gained. Finally, the ^{15}N labeling of capsicein that was imposed by the numerous overlaps opens the possibility to study the interactions of this protein with biological partners, among which lipids and membranes seem to play an important role.

REFERENCES

Anderson, A. J., Rogers, K., Tepper, C. S., & Blee, K. (1991) *Physiol. Mol. Plant Pathol. 38*, 1–13.

Aue, W. P., Bartholdi, E., & Ernst, R. R. (1976) *J. Chem. Phys. 64*, 2229–2246.

Bax, A., Griffey, R. H., & Hawkins, B. L. (1983) *J. Magn. Reson. 55*, 301–315.

Blein, J. P., Milat, M. L., & Ricci, P. (1991) *Plant Physiol. 95*, 486–491.

Braunschweiler, L., & Ernst, R. R. (1983) *J. Magn. Reson. 53*, 521–528.

Brooks, B. R., Bruccoleri, R. E., Olafson, B. D., States, D. J., Swaminathan, S., & Karplus, M. (1983) *J. Comput. Chem. 4*, 187–217.

Brown, S. C., Weber, P. L., & Mueller, L. (1988) *J. Magn. Reson. 77*, 166–169.

Brünger, A., Clore, G. M., Gronenborn, A. M., & Karplus, M. (1986) *Proc. Natl. Acad. Sci. U.S.A. 83*, 3801–3805.

Brünger, A. T. (1992) *XPLOR Manual*, Yale University, New Haven, CT.

Bystrov, V. F. (1976) *Prog. Nucl. Magn. Reson. Spectrosc. 10*, 41–81.

Dixon, R. A., & Lamb, C. J. (1990) *Annu. Rev. Plant Physiol. Plant Mol. Biol. 41*, 339–367.

Englander, S. W., & Wand, A. J. (1987) *Biochemistry 26*, 5953–5958.

Farmer, E. E., & Ryan, C. A. (1992) *Trends Cell Biol. 2*, 236–241.

Fesik, S. W., & Zuiderweg, E. R. P. (1988) *J. Magn. Reson. 78*, 588–593.

Frenkiel, T., Bauer, C., Carr, M. D., Birsall, B., & Feeney, J. (1990) *J. Magn. Reson. 90*, 420–425.

Griesinger, C., Sørensen, O. W., & Ernst, R. R. (1987) *J. Magn. Reson. 73*, 574–579.

Gronenborn, A. M., Bax, A., Wingfield, P. T., & Clore, G. M. (1989) *FEBS Lett. 243*, 93–98.

Güntert, P., Braun, W., Billeter, M., & Wüthrich, K. (1989) *J. Am. Chem. Soc. 111*, 3997–4004.

Güntert, P., Braun, W., & Wüthrich, K. (1991) *J. Mol. Biol. 217*, 517–530.

Hahlbrock, K., Gross, P., Colling, C., & Scheel, D. (1990) in *Plant Molecular Biology* (Hermann, R. G., & Larkils, B. A., Eds.) pp 147–151, Plenum Press, New York.

Huet, J. C., & Pernollet, J. C. (1993) *Phytochemistry 33*, 797–805.

Huet, J. C., Nespoulous, C., & Pernollet, J. C. (1992) *Phytochemistry 31*, 1471–1476.

Huet, J. C., Mansion, M., & Pernollet, J. C. (1993) *Phytochemistry 34*, 1261–1264.

Huet, J. C., Sallé-Tourne, M., & Pernollet, J. C. (1994) *Mol. Plant-Microbe Interact. 7*, 302–304.

Ikura, M., Bax, A., Clore, G. M., & Gronenborn, G. M. (1990) *J. Am. Chem. Soc. 112*, 9020–9022.

Jeener, J., Meir, B. H., Bachmann, P., & Ernst, R. R. (1979) *J. Chem. Phys. 71*, 4546–4553.

Kamoun, S., Young, M., Glascock, C. B., & Tyler, B. M. (1993) *Mol. Plant-Microbe Interact. 6*, 15–25.

Karplus, M. (1959) *J. Chem. Phys. 30*, 11–15.

Ludvigsen, S., Anderson, K. V., & Poulsen, F. M. (1991) *J. Mol. Biol. 217*, 731–736.

Marion, D., Kay, L. E., Sparks, S. W., Torchia, D. A., & Bax, A. (1989a) *J. Am. Chem. Soc. 111*, 1515–1517.

Marion, D., Driscoll, P. C., Kay, L. E., Wingfield, P. T., Bax, A., Gronenborn, A. M., & Clore, G. M. (1989b) *Biochemistry 28*, 6150–6156.

Mueller, L. (1979) *J. Am. Chem. Soc. 101*, 4481–4484.

Nespoulous, C., Huet, J. C., & Pernollet, J. C. (1992) *Planta 186*, 551–557.

Pardi, A., Billeter, M., & Wüthrich, K. (1984) *J. Mol. Biol. 180*, 741–751.

Pernollet, J. C., Sallantin, M., Sallé-Tourné, M., & Huet, J. C. (1993) *Physiol. Mol. Plant Pathol. 42*, 53–67.

Redfield, A. G., & Kuntz, S. D. (1975) *J. Magn. Reson. 19*, 250–254

Ricci, P., Bonnet, P., Huet, J. C., Sallantin, M., Beauvais-Cante, F., Bruneteau, M., Billard, V., Michel, G., & Pernollet, J. C. (1989) *Eur. J. Biochem. 183*, 555–563.

Scott, D. L., & Sigler, P. B. (1994) *Adv. Protein Chem. 45*, 53–88.

Sembdner, G., & Parthier, B. (1993) *Annu. Rev. Plant Physiol. Plant Mol. Biol. 44*, 569–589.

Shaka, A. J., Barker, P. B., & Freeman, R. (1985) *J. Magn. Reson. 64*, 547–552.

Sklenár, V., & Bax, A. (1987) *J. Magn. Reson. 71*, 379–383.

Tercé-Laforgue, T., Huet, J. C., & Pernollet, J. C. (1992) *Plant Physiol. 98*, 936–941.

Vuister, G. W., Boelens, R., & Kaptein, R. (1988) *J. Magn. Reson. 80*, 176–185.

Wagner, G., Braun, W., Havel, T. F., Schaumann, T., Gō, N., & Wüthrich, K. (1987) *J. Mol. Biol. 196*, 611–639.

Wand, A. J., & Nelson, S. J. (1988) Refinement and automation of the main chain directed assignment of 1H spectra of proteins, *Trans. Am. Crystallogr. Assoc. 24*, 131–144.

Wüthrich, K. (1986) *NMR of proteins and nucleic acids*, John Wiley, New York.

Zanetti, A., Beauvais, F., Huet, J. C., & Pernollet, J. C. (1992) *Planta 187*, 163–170.

Zuiderwerg, E. R. P., Boelens, R., & Kaptein, R. (1985) *Biopolymers 24*, 601–611.